

Nonequilibrium many-body quantum engine driven by time-translation symmetry breaking

Federico Carollo,¹ Kay Brandner,² and Igor Lesanovsky^{1,2}

¹*Institut für Theoretische Physik, Universität Tübingen,
Auf der Morgenstelle 14, 72076 Tübingen, Germany*

²*School of Physics and Astronomy and
Centre for the Mathematics and Theoretical Physics of Quantum Non-Equilibrium Systems,
University of Nottingham, Nottingham, NG7 2RD, UK*

(Dated: January 3, 2022)

Quantum many-body systems out of equilibrium can host intriguing phenomena such as transitions to exotic dynamical states. Although this emergent behaviour can be observed in experiments, its potential for technological applications is largely unexplored. Here, we investigate the impact of collective effects on quantum engines that extract mechanical work from a many-body system. Using an opto-mechanical cavity setup with an interacting atomic gas as a working fluid, we demonstrate theoretically that such engines produce work under periodic driving. The stationary cycle of the working fluid features nonequilibrium phase transitions, resulting in abrupt changes of the work output. Remarkably, we find that our many-body quantum engine operates even without periodic driving. This phenomenon occurs when its working fluid enters a phase that breaks continuous time-translation symmetry: the emergent time-crystalline phase can sustain the motion of a load generating mechanical work. Our findings pave the way for designing novel nonequilibrium quantum machines.

Future-generation nanomachines will require powerful small-scale engines whose energy output can be channeled into mechanical work storages. Proof-of-principle experiments have shown how such microscopic flywheels can be realized for working systems with few internal degrees of freedom like a single atom [1–5]. Yet it is less clear how the output of a quantum engine can be converted into motive power if its working fluid consists of a many-body system.

During the last years, much progress has been made in the design of quantum engines that operate far from equilibrium and use non-thermal sources of energy [6–12]. The natural next step is to explore how mechanical work can be generated in such non-equilibrium settings, how collective effects, like phase transitions, affect the work output and whether they could enable novel modes of operation.

In this article, we propose a new type of many-body quantum engine, that is driven by time-translation symmetry breaking [13–15] and does not require a periodic protocol. Our engine autonomously delivers mechanical work to an external load as a result of its working fluid hosting a phase with broken (continuous) time-translation symmetry, a so-called time crystal [13–15]. We show that such an exotic device can be implemented with a general cavity-atom setting, which can, in principle, be realized in experiments with cold atoms [16–18], see the sketch in Fig.1. In this setup, one mirror of the cavity is fixed, while the other one is attached to a micro-spring and can move around its equilibrium position [19–21]. By driving the atoms inside the cavity with a periodically modulated laser, the free mirror can be forced into sustained oscillations from which we determine the work delivered by the engine [22–25].

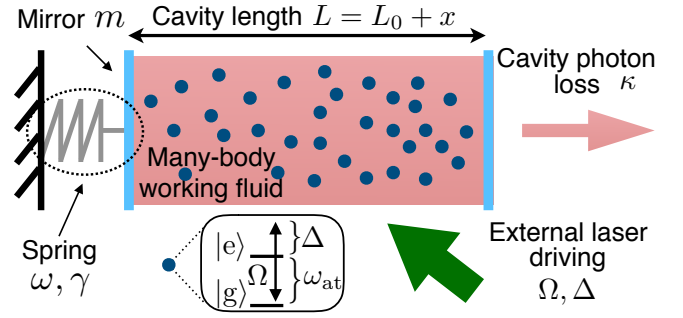


FIG. 1. Cavity-atom quantum engine. The atomic working fluid is held in an optical cavity with one movable mirror (mass m) attached to a spring (characteristic frequency ω). The cavity length $L = L_0 + x$ decomposes into an equilibrium length L_0 and a small deviation x . The motion of the mirror is damped by mechanical friction (proportional to the coefficient γ) and driven by thermal fluctuations and the radiation pressure inside the cavity. Each atom is described as a two-level system with ground state $|g\rangle$, excited state $|e\rangle$ and energy splitting ω_{at} . Excitations are generated and destroyed through interactions with a light mode in the cavity and with the driving laser (Rabi frequency Ω and detuning Δ). The cavity loss rate is κ .

Our numerical analysis reveals two quite remarkable effects. First, the system features a series of nonequilibrium phase transitions leading to sudden changes of the asymptotic cycle. Second, even in the absence of an explicit periodic driving, where one would *a priori* expect the system to approach to a stationary state, the oscillatory motion of the mirror can be sustained as the atomic working fluid forms a time-crystalline phase [13–15] for properly chosen parameters.

Beyond illuminating these intriguing many-body

effects, our approach has the key advantage that it admits a clear thermodynamic interpretation. Since the mirror is effectively classical, its position can be monitored without disturbing the operation cycle of the engine, thus avoiding the subtleties of measuring a quantum working fluid. Such quasi-classical work measurements make it possible to unambiguously determine the effective output of a quantum engine. At the same time, they open new ways to probe collective phenomena in nonequilibrium quantum many-body systems.

Cavity-atom setup.— We consider the setup of Fig. 1. An ensemble of N atoms is loaded into an optical cavity with one movable mirror. Each atom is described as a two-level system with ground state $|g\rangle$, excited state $|e\rangle$, and level splitting ω_{at} . A single light mode is resonant with the cavity at frequency ω_{cav} . The exchange of photons between atoms and light field is described by the coupling Hamiltonian

$$H_{\text{int}} = \hbar \frac{g}{\sqrt{N}} (a S_+ + a^\dagger S_-) \quad \text{with} \quad S_\pm = \sum_{k=1}^N \sigma_\pm^{(k)}. \quad (1)$$

Here, a and a^\dagger are the photon creation and annihilation operators and $\sigma_- = |g\rangle\langle e|$ and $\sigma_+ = \sigma_-^\dagger$ are the atomic transition operators. The interaction strength is rescaled by the factor $1/\sqrt{N}$ as is common for light-matter interactions of this type [26–28]. The atoms are further driven by an external laser, whose frequency is shifted from ω_{at} by the detuning Δ . In the rotating frame of the laser, the atomic Hamiltonian is given by [18, 29–31]

$$H_L = \hbar \left[\Omega (S_+ + S_-) - \frac{\Delta}{2} S_z \right] \quad \text{with} \quad S_z = \sum_{k=1}^N \sigma_z^{(k)}, \quad (2)$$

where $\sigma_z = |e\rangle\langle e| - |g\rangle\langle g|$. The Rabi frequency Ω is determined by the strength of the coherent driving. In the same rotating frame, the free Hamiltonian of the light field reads $H_{\text{ph}} = -\hbar\delta a^\dagger a$, where $\delta = \omega_{\text{at}} + \Delta - \omega_{\text{cav}}$ is the effective detuning of the cavity mode. The loss of photons from the cavity, at rate κ , is described by the dissipation super operator [32–35]

$$\mathcal{D}_{\text{ph}}[\rho] = \hbar\kappa \left(a\rho a^\dagger - \frac{1}{2} \{ \rho, a^\dagger a \} \right).$$

In the Schrödinger picture, the bare photon Hamiltonian is given by $H_{\text{ph}}^S = \hbar\omega_{\text{cav}} a^\dagger a$. The frequency of the photons is connected to the length L of the cavity through the resonance condition $\omega_{\text{cav}} = nc/(2L)$ with n being an integer and c the speed of light. We decompose the length of the cavity, $L = L_0 + x$, into an equilibrium contribution L_0 and a deviation x , which accounts for small oscillations of the first mirror, see Fig. 1. Expanding the

Hamiltonian H_{ph}^S to first order in x/L_0 yields [19–21]

$$H_{\text{ph}}^S \approx \hbar\omega_{\text{cav}}^0 \left(1 - \frac{x}{L_0} \right) a^\dagger a \quad \text{with} \quad \omega_{\text{cav}}^0 = \frac{nc}{2L_0}. \quad (3)$$

This result shows that the position of the mirror and the number of photons are coupled [19–21]. In fact, the Hamiltonian in Eq. (3) describes a mechanical force on the mirror, which emerges from the radiation pressure inside the cavity.

In addition, the light field in the cavity mediates an effective excitation-exchange coupling between the atoms, which arises from the interaction Hamiltonian (1) when the electromagnetic field is traced out [36, 37]. In the weak-coupling regime $\kappa \gg g/\sqrt{N}$, the state of the atoms ρ_t follows an effective Lindblad equation [17, 32–35, 38]

$$\dot{\rho}_t = -\frac{i}{\hbar} [\tilde{H}, \rho_t] + \frac{1}{\hbar} \tilde{\mathcal{D}}[\rho_t]. \quad (4)$$

Upon neglecting second-order contributions in the relative displacement x/L_0 , the corresponding effective Hamiltonian and dissipation super-operator become

$$\tilde{H} = H_L + \frac{\hbar g}{N} \left(C_0 - \frac{C_1}{L_0} x \right) S_+ S_-, \quad (5)$$

and

$$\tilde{\mathcal{D}}[\rho] = \frac{\hbar g}{N} \left(\Gamma_0 - \frac{\Gamma_1}{L_0} x \right) \left(S_- \rho S_+ - \frac{1}{2} \{ \rho, S_+ S_- \} \right), \quad (6)$$

with the dimensionless constants [38]

$$C_0 = \frac{4\delta_0 g}{\kappa^2 + 4\delta_0^2}, \quad \Gamma_0 = \frac{4\kappa g}{\kappa^2 + 4\delta_0^2}, \\ C_1 = \frac{\omega_{\text{cav}}^0}{\delta_0} C_0 \frac{4\delta_0^2 - \kappa^2}{4\delta_0^2 + \kappa^2}, \quad \Gamma_1 = \omega_{\text{cav}}^0 \Gamma_0 \frac{8\delta_0}{\kappa^2 + 4\delta_0^2}$$

and the detuning parameter $\delta_0 = \omega_{\text{at}} + \Delta - \omega_{\text{cav}}^0$.

Dynamics of the mirror.— The mirror is a massive object, whose ground state energy is small compared to the typical energy of thermal excitations. That is, we have $\hbar\omega \ll k_B T$, where ω is the characteristic frequency of the spring attached to the mirror, see Fig. 1, and T is the base temperature of the setup. The position of the mirror can thus be treated as a classical degree of freedom, whose dynamics is governed by the Langevin equation [25, 39]

$$m\ddot{x} + \gamma\dot{x} + m\omega^2 x = f_t + \xi_t; \quad (7)$$

here, γ is the damping coefficient, m is the mass of the mirror and the stochastic force ξ_t , which describes thermal fluctuations, obeys $\mathbb{E}[\xi_t] = 0$ and $\mathbb{E}[\xi_t \xi_s] = 2\gamma k_B T \delta(t - s)$. The symbol \mathbb{E} indicates average over all realizations [40].

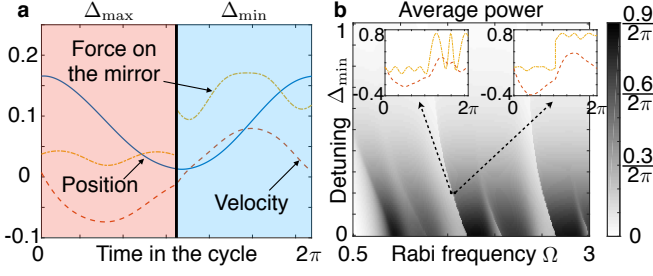


FIG. 2. **Periodic driving.** (a) Periodic motion of the mirror driven by the many-body engine. The average velocity of the mirror, \bar{v}_t , is given in units of $v_0 = \frac{\omega_{\text{cav}}^0}{\omega} \frac{\hbar D_0}{m}$, the average position, \bar{x}_t , in units of v_0/ω and the force in units of $\hbar\omega_{\text{cav}}^0 D_0$. Time is given in units of ω^{-1} . This representative cycle is obtained for $\omega_{\text{at}} - \omega_{\text{cav}}^0 = 0.1\omega$, $\Delta_{\max} = 2\omega$ and $\Delta_{\min} = \kappa = g = \omega$. The mean velocity is non-zero, proving that the engine constantly delivers energy to the mirror through the force f_t . (b) Power output, in units of $mv_0^2\omega$, as a function of Ω/ω and Δ_{\min}/ω with fixed $\Delta_{\max} - \Delta_{\min} = \omega$. In the insets, we show the mean velocity and the force for $\Delta_{\min} = 0.2\omega$ and two slightly different values of the Rabi frequency, $\Omega/\omega = 1.55, 1.56$, for which the power output differs substantially. The force profile changes abruptly from an oscillatory pattern to a two plateau-like shape indicating a non-equilibrium phase transition. Numerical results have been obtained by simulating the dynamics of the mirror for sufficiently long times, such that the system has converged to its asymptotic cycle.

The deterministic force $f_t = -\langle \left[\frac{\partial}{\partial x} H_{\text{ph}}^S \right] \rangle_t$ is due to the light-mediated coupling between the mirror and the working fluid. In the effective picture of an interacting atomic gas, it is, up to second-order corrections in the displacement of the mirror x/L_0 , given by [38],

$$f_t \approx \hbar \frac{g}{N} \frac{\omega_{\text{cav}}^0}{\kappa L_0} \left(\Gamma_0 - \Gamma_1 \frac{x}{L_0} \right) \langle S_+ S_- \rangle_t, \quad (8)$$

where angular brackets denote the average with respect to the state of the atomic system ρ_t . Together with this relation, the effective master equation (4) and the Langevin equation (7) determine the joint dynamics of the mirror and the working fluid.

Finite-density limit.— We now consider the limit of large atom numbers, $N \gg 1$, focussing on the case where the linear density of atoms in the cavity, $D_0 = N/L_0$, is fixed. This assumption, which is typically well justified in experiments, makes it possible to simplify our mathematical model. First, the constants C_1 and Γ_1 , appearing in Eqs. (5)-(6), become irrelevant for the dynamics, as they are of order N^{-2} , and can thus be neglected. Second, the normalized correlation functions $\langle S_+ S_- \rangle/N^2$ factorize, since emergent correlations between different atoms are wiped out in the large- N limit [41, 42]. That is, we have $\langle S_+ S_- \rangle/N^2 \sim s_+ s_-$ with $s_{\pm} = \lim_{N \rightarrow \infty} \langle S_{\pm} \rangle/N$.

As a result, the collective atomic variables s_{\pm} and

$s_z = \lim_{N \rightarrow \infty} \langle S_z \rangle/N$ obey the mean-field type dynamical equations [38, 42]

$$\begin{aligned} \dot{s}_+ &= -i\Omega s_z - i\Delta s_+ - igC_0 s_z s_+ + \frac{g_0 \Gamma_0}{2} s_z s_+, \\ \dot{s}_z &= 2i\Omega (s_- - s_+) - 2g\Gamma_0 s_+ s_-, \end{aligned} \quad (9)$$

and the Langevin equation (7) becomes

$$m\ddot{x} + \gamma\dot{x} + m\omega^2 x = \hbar \frac{g\omega_{\text{cav}}^0 \Gamma_0 D_0}{\kappa} s_+ s_- + \xi_t; \quad (10)$$

since the expression (8) for the deterministic force reduces to

$$f_t = \hbar \frac{g\omega_{\text{cav}}^0 \Gamma_0 D_0}{\kappa} s_+ s_- \quad (11)$$

in the thermodynamic limit. The Eqs.(9)-(10) provide a complete dynamical model of our engine in terms of the four variables s_{\pm} , s_z and x .

Work extraction through the mirror.— We first consider a conventional isothermal engine cycle, where the detuning Δ is periodically modulated to provide energy input. For simplicity, we focus on a quench protocol, where $\Delta = \Delta_{\max}$ during the first half of the period and $\Delta = \Delta_{\min}$ during the second half, as shown in Fig. 2(a). The period t_c of the driving is resonant with the eigenfrequency of the mirror, $t_c = 2\pi/\omega$. As a consequence of the driving, the state of the atoms ρ_t and the average position of the mirror approach an asymptotic cycle with period t_c . As initial conditions we consider all atoms in their ground state and the mirror in its equilibrium position ($x_0 = \dot{x}_0 = 0$). However, at least at a qualitative level, our results do not depend on the specific initial conditions.

Owing to energy conservation, the average amount of work that is transferred from the atomic system to the mirror plus the energy contribution of the thermal fluctuations must be equal to the average heat dissipation due to mechanical friction. Hence, the power delivered by the engine per cycle is given by

$$P_{\text{av}} = \frac{\gamma}{t_c} \int_0^{t_c} dt \left(\mathbb{E} [v_t^2] - \frac{k_B T}{m} \right) = \frac{\gamma}{t_c} \int_0^{t_c} dt \bar{v}_t^2, \quad (12)$$

as shown in Methods by using tools of stochastic thermodynamics. Here, $v_t = \dot{x}_t$ is the velocity of the mirror, $\gamma k_B T/m$ represents the thermal energy dissipated by mechanical friction, and \bar{v}_t is the average velocity of the mirror—which can be obtained from Eq. (10) with $\xi_t = 0$.

In Fig. 2(b), the generated mean power P_{av} is plotted as a function of the Rabi frequency Ω and the lower level of the detuning Δ_{\min} . We find that P_{av} is positive over a large range of parameters. This result proves that our engine is able to produce usable work by sustaining the

periodic motion of the mirror against constant damping. Quite remarkably, the average power output features discontinuous jumps signalling nonequilibrium phase transitions in the asymptotic periodic state as illustrated by the insets of Fig. 2(b). This new type of phase transition generalizes steady-state nonequilibrium ones to periodically driven settings. The power output acts as an order parameter which can be used to unveil the occurrence of sudden changes in the asymptotic periodic dynamics of the many-body working fluid.

Time-translation symmetry breaking.— Once the time-dependent modulation of the detuning is turned off, one would expect the mirror to come to rest as the working fluid settles to a steady state. However, our analysis shows that, for properly chosen parameters, the engine still drives sustained oscillations of the mirror, even if the detuning is fixed. This *a priori* surprising phenomenon arises as a consequence of the working fluid entering a time-crystal phase, which breaks the continuous temporal translation symmetry of the time-independent generator of the dynamics [15]. The engine thereby acquires a new operation mechanism, which does not require cyclic control protocols and instead makes it possible to generate periodic motion from steady-state driving, as illustrated in Fig. 3(a).

In the absence of a periodic protocol, there is no natural recurrence time for the long-time dynamics which, in general, may or may not approach an asymptotic cycle. To explore this regime quantitatively, we thus need to determine the average power of the engine by calculating the average heat loss generated by the mirror over a long time window. Namely, we compute the power as

$$P_{\text{av}} = \lim_{t_{\text{obs}} \rightarrow \infty} \frac{\gamma}{t_{\text{obs}}} \int_0^{t_{\text{obs}}} dt \bar{v}_t^2.$$

If the position of the mirror settles on an asymptotic cycle with a well-defined period, this definition coincides with the one given in Eq. (12).

The results of our analysis are summarized in Fig. 3(b). In the weak photon-loss regime, i.e. for $\kappa \ll \Omega$, the working fluid settles to a stationary state where no mechanical work is produced. Approximately at $\kappa \sim 1/\Omega$, for the specific choice of parameters, a phase transition occurs and the average power abruptly increases as the mirror breaks into sustained oscillations. This effect is most pronounced at moderate photon-loss rates, where our time-crystal engine delivers the largest output.

The working mechanism of this new operation mode of the engine can be understood as follows. The effective dissipation constant Γ_0 decays with large photon-loss rates κ . In this regime, characterized by weak dissipation on the atoms ($\Gamma_0 \ll 1$), the dynamics of the working fluid is dominated by the Rabi driving at frequency Ω . As a result, the steady-state manifold of the atomic system becomes degenerate and long-lived oscillations

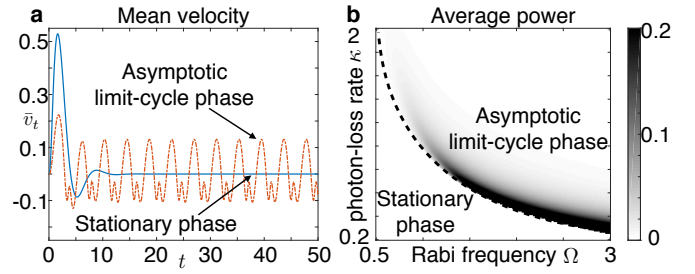


FIG. 3. Time-crystal quantum engine. (a) Mean velocity of the mirror in units of $v_0 = \frac{\omega_{\text{cav}}^0}{\omega} \frac{\hbar D_0}{m}$ as a function of time (in units of ω^{-1}) for two different photon-loss rates. For $\kappa/\omega = 0.5$, the mirror comes to rest while sustained oscillations emerge for $\kappa/\omega = 1.5$. For this plot we have set $\Delta = 0$, $\omega_{\text{at}} - \omega_{\text{cav}}^0 = 0.1\omega$ and $\Omega = g = \omega$. (b) Average power output, in units of $m v_0^2 \omega$, as a function of the photon-loss rate κ and the Rabi frequency Ω , both in units of ω . Along the dashed line $\kappa\Omega \sim 1$, a phase transition occurs, where the average power jumps to a finite value as the working fluid spontaneously forms a time crystal. The scale has been truncated at 0.2, but significantly larger values for the work output ($P_{\text{av}} > 2$) are found. The maximum value, for the chosen parameters, is given by $P_{\text{av}} \sim 2.8$.

within this manifold emerge [15]. Thus, oscillating coherences are responsible for the time-dependent force on the mirror. When atomic dissipation dominates, coherent oscillations are suppressed and the working fluid approaches a time-invariant steady-state. In this case, the radiation pressure on the mirror is constant and the mirror comes to rest.

Discussion.— We have developed a general framework for the dynamical description of many-body quantum engines, which includes the external load as a semi-classical degree of freedom. This approach makes it possible to determine the performance of the engine directly by monitoring the coupled dynamics of both the working fluid and of the load.

This perspective allowed us to obtain two key results. First, in the periodic mode of operation, where the engine is driven by modulations of an external control parameter, a new type of nonequilibrium phase transitions emerges. The power output of the engine thereby plays the role of an order parameter.

Second, we have demonstrated that, even when the engine is not driven through a periodic protocol, and is thus described by a time-independent generator, it can still deliver mechanical work. The emergence of this new regime is due to a nonequilibrium phase transition in the atomic working fluid towards an exotic state that features sustained coherent oscillations. This dynamical time-crystalline phase [13–15] can drive the motion of the load without relying on a time-dependent control protocol. Our approach paves the way to explore new mechanisms of power generation enabled by collective many-

body effects and, at the same time, provides a natural description of many-body quantum engines.

Our predictions on the power output of our engine can be tested with current technology in cavity-atom experiments [16, 17, 43–45], and our general numerical analysis covers a wide range of different setups.

FC acknowledges support through a Teach@Tübingen Fellowship. KB received support from the University of Nottingham through a Nottingham Research Fellowship and from UK Research and Innovation through a Future Leaders Fellowship (Grant Reference: MR/S034714/1). IL acknowledges support from the DFG through SPP 1929 (GiRyd) as well as from the “Wissenschaftler-Rückkehrprogramm GSO/CZS” of the Carl-Zeiss-Stiftung and the German Scholars Organization e.V.

-
- [1] Holger Thierschmann, Rafael Sánchez, Björn Sothmann, Fabian Arnold, Christian Heyn, Wolfgang Hansen, Hartmut Buhmann, and Laurens W. Molenkamp, “Three-terminal energy harvester with coupled quantum dots,” *Nature Nanotechnology* **10**, 854–858 (2015).
 - [2] Johannes Roßnagel, Samuel T. Dawkins, Karl N. Tolazzi, Obinna Abah, Eric Lutz, Ferdinand Schmidt-Kaler, and Kilian Singer, “A single-atom heat engine,” *Science* **352**, 325 (2016).
 - [3] Martin Josefsson, Artis Svilans, Adam M. Burke, Eric A. Hoffmann, Sofia Fahlvik, Claes Thelander, Martin Leijnse, and Heiner Linke, “A quantum-dot heat engine operating close to the thermodynamic efficiency limits,” *Nature Nanotechnology* **13**, 920–924 (2018).
 - [4] D. von Lindenfels, O. Gräß, C. T. Schmiegelow, V. Kaushal, J. Schulz, Mark T. Mitchison, John Goold, F. Schmidt-Kaler, and U. G. Poschinger, “Spin heat engine coupled to a harmonic-oscillator flywheel,” *Phys. Rev. Lett.* **123**, 080602 (2019).
 - [5] John P. S. Peterson, Tiago B. Batalhão, Marcela Herrera, Alexandre M. Souza, Roberto S. Sarthour, Ivan S. Oliveira, and Roberto M. Serra, “Experimental characterization of a spin quantum heat engine,” *Phys. Rev. Lett.* **123**, 240601 (2019).
 - [6] Cyril Elouard, David Herrera-Martí, Benjamin Huard, and Alexia Auffèves, “Extracting work from quantum measurement in Maxwell’s Demon engines,” *Phys. Rev. Lett.* **118**, 260603 (2017).
 - [7] Cyril Elouard and Andrew N. Jordan, “Efficient quantum measurement engines,” *Phys. Rev. Lett.* **120**, 260601 (2018).
 - [8] Wolfgang Niedenzu and Gershon Kurizki, “Cooperative many-body enhancement of quantum thermal machine power,” *New Journal of Physics* **20**, 113038 (2018).
 - [9] Marco Pezzutto, Mauro Paternostro, and Yasser Omar, “An out-of-equilibrium non-Markovian quantum heat engine,” *Quantum Science and Technology* **4**, 025002 (2019).
 - [10] Nicole Yunger Halpern, Christopher David White, Sarang Gopalakrishnan, and Gil Refael, “Quantum engine based on many-body localization,” *Phys. Rev. B* **99**, 024203 (2019).
 - [11] Najmeh Etehadi Abari, Giulia Vittoria De Angelis, Stefano Zippilli, and David Vitali, “An optomechanical heat engine with feedback-controlled in-loop light,” *New Journal of Physics* **21**, 093051 (2019).
 - [12] Federico Carollo, Filippo M. Gambetta, Kay Brandner, Juan P. Garrahan, and Igor Lesanovsky, “Nonequilibrium quantum many-body Rydberg atom engine,” *Phys. Rev. Lett.* **124**, 170602 (2020).
 - [13] Frank Wilczek, “Quantum time crystals,” *Phys. Rev. Lett.* **109**, 160401 (2012).
 - [14] Alfred Shapere and Frank Wilczek, “Classical time crystals,” *Phys. Rev. Lett.* **109**, 160402 (2012).
 - [15] F. Iemini, A. Russomanno, J. Keeling, M. Schirò, M. Dalmonte, and R. Fazio, “Boundary time crystals,” *Phys. Rev. Lett.* **121**, 035301 (2018).
 - [16] Matthew A. Norcia, Matthew N. Winchester, Julia R. K. Cline, and James K. Thompson, “Superradiance on the millihertz linewidth strontium clock transition,” *Science Advances* **2** (2016), 10.1126/sciadv.1601231.
 - [17] Matthew A. Norcia, Robert J. Lewis-Swan, Julia R. K. Cline, Bihui Zhu, Ana M. Rey, and James K. Thompson, “Cavity-mediated collective spin-exchange interactions in a strontium superradiant laser,” *Science* **361**, 259–262 (2018).
 - [18] Helmut Ritsch, Peter Domokos, Ferdinand Brennecke, and Tilman Esslinger, “Cold atoms in cavity-generated dynamical optical potentials,” *Rev. Mod. Phys.* **85**, 553–601 (2013).
 - [19] Markus Aspelmeyer, Tobias J. Kippenberg, and Florian Marquardt, “Cavity optomechanics,” *Rev. Mod. Phys.* **86**, 1391–1452 (2014).
 - [20] Keye Zhang, Francesco Bariani, and Pierre Meystre, “Quantum optomechanical heat engine,” *Phys. Rev. Lett.* **112**, 150602 (2014).
 - [21] M Brunelli, A Xuereb, A Ferraro, G De Chiara, N Kiesel, and M Paternostro, “Out-of-equilibrium thermodynamics of quantum optomechanical systems,” *New Journal of Physics* **17**, 035016 (2015).
 - [22] Ken Sekimoto, “Kinetic characterization of heat bath and the energetics of thermal ratchet models,” *Journal of the Physical Society of Japan*, *Journal of the Physical Society of Japan* **66**, 1234–1237 (1997).
 - [23] Ken Sekimoto, “Langevin Equation and Thermodynamics,” *Progress of Theoretical Physics Supplement* **130**, 17–27 (1998).
 - [24] Ken Sekimoto, *Stochastic energetics*, Vol. 799 (Springer, Berlin, 2010).
 - [25] Udo Seifert, “Stochastic thermodynamics, fluctuation theorems and molecular machines,” *Reports on Progress in Physics* **75**, 126001 (2012).
 - [26] Klaus Hepp and Elliott H. Lieb, “Equilibrium statistical mechanics of matter interacting with the quantized radiation field,” *Phys. Rev. A* **8**, 2517–2525 (1973).
 - [27] Klaus Hepp and Elliott H. Lieb, “On the superradiant phase transition for molecules in a quantized radiation field: the Dicke maser model,” *Annals of Physics* **76**, 360–404 (1973).
 - [28] Peter Kirton, Mor M. Roses, Jonathan Keeling, and Emanuele G. Dalla Torre, “Introduction to the Dicke model: From equilibrium to nonequilibrium, and vice versa,” *Advanced Quantum Technologies* **2**, 1800043 (2019).
 - [29] Christoph Hamsen, Karl Nicolas Tolazzi, Tatjana Wilk,

- and Gerhard Rempe, “Two-photon blockade in an atom-driven cavity QED system,” *Phys. Rev. Lett.* **118**, 133604 (2017).
- [30] Rahul Sawant and S. A. Rangwala, “Lasing by driven atoms-cavity system in collective strong coupling regime,” *Scientific Reports* **7**, 11432 (2017).
- [31] Tony E. Lee, H. Häffner, and M. C. Cross, “Collective quantum jumps of Rydberg atoms,” *Phys. Rev. Lett.* **108**, 023602 (2012).
- [32] G. Lindblad, “On the generators of quantum dynamical semigroups,” *Comm. Math. Phys.* **48**, 119–130 (1976).
- [33] Vittorio Gorini, Andrzej Kossakowski, and Ennackal Chandy George Sudarshan, “Completely positive dynamical semigroups of N-level systems,” *Journal of Mathematical Physics* **17**, 821–825 (1976).
- [34] H.P. Breuer and F. Petruccione, *The theory of open quantum systems* (Oxford University Press, 2002).
- [35] Crispin Gardiner and Peter Zoller, *Quantum noise* (Springer, 2004).
- [36] G. S. Agarwal, R. R. Puri, and R. P. Singh, “Atomic schrödinger cat states,” *Phys. Rev. A* **56**, 2249–2254 (1997).
- [37] Sarang Gopalakrishnan, Benjamin L. Lev, and Paul M. Goldbart, “Frustration and glassiness in spin models with cavity-mediated interactions,” *Phys. Rev. Lett.* **107**, 277201 (2011).
- [38] See supplemental material for details..
- [39] Mohammad Yaghoubi, M Ebrahim Foulaadvand, Antoine Bérut, and Jerzy Luczka, “Energetics of a driven brownian harmonic oscillator,” *Journal of Statistical Mechanics: Theory and Experiment* **2017**, 113206 (2017).
- [40] Hannes Risken, *The Fokker-Planck Equation* (Springer, Berlin, 1996).
- [41] F. Benatti, F. Carollo, R. Floreanini, and H. Narnhofer, “Non-Markovian mesoscopic dissipative dynamics of open quantum spin chains,” *Physics Letters A* **380**, 381 – 389 (2016).
- [42] F Benatti, F Carollo, R Floreanini, and H Narnhofer, “Quantum spin chain dissipative mean-field dynamics,” *Journal of Physics A: Mathematical and Theoretical* **51**, 325001 (2018).
- [43] Igor B. Mekhov, Christoph Maschler, and Helmut Ritsch, “Probing quantum phases of ultracold atoms in optical lattices by transmission spectra in cavity quantum electrodynamics,” *Nature Physics* **3**, 319–323 (2007).
- [44] Ferdinand Brennecke, Stephan Ritter, Tobias Donner, and Tilman Esslinger, “Cavity optomechanics with a Bose-Einstein condensate,” *Science* **322**, 235–238 (2008).
- [45] Kristian Baumann, Christine Guerlin, Ferdinand Brennecke, and Tilman Esslinger, “Dicke quantum phase transition with a superfluid gas in an optical cavity,” *Nature* **464**, 1301–1306 (2010).

METHODS

Stochastic dynamics of the mirror in the finite-density regime. Owing to its large mass, the mirror can be described as a classical oscillator, which is driven by the force from the atoms and subject to thermal fluctuations due to its environment having a finite temperature T . The displacement x of the mirror from its equilibrium

position follows the underdamped Langevin equation [25] in Eq. (10). The systematic force f_t stems from the radiation pressure inside the cavity and is related to the state of the atoms via the expression (11).

A convenient way to solve Eq. (10), is to rewrite it as a system of first-order differential equations,

$$\frac{d}{dt} \begin{pmatrix} x_t \\ v_t \end{pmatrix} = \begin{pmatrix} 0 & 1 \\ -\omega^2 & -2\gamma_0 \end{pmatrix} \begin{pmatrix} x_t \\ v_t \end{pmatrix} + \frac{1}{m} \begin{pmatrix} 0 \\ f_t + \xi_t \end{pmatrix} \quad (13)$$

where $v_t = \dot{x}_t$ and $\gamma_0 = \gamma/(2m)$. Upon introducing the vector notation

$$\vec{x}_t = \begin{pmatrix} x_t \\ v_t \end{pmatrix}, \quad \vec{G}_t = \frac{1}{m} \begin{pmatrix} 0 \\ f_t \end{pmatrix}, \quad M = \begin{pmatrix} 0 & 1 \\ -\omega^2 & -2\gamma_0 \end{pmatrix},$$

the formal solution of Eq. (13) can be written as

$$\vec{x}_t = e^{tM} \vec{x}_0 + \int_0^t ds e^{(t-s)M} \vec{G}_s.$$

With initial conditions $x_0 = v_0 = 0$, we have

$$x_t = \bar{x}_t + x_t^\xi,$$

where (defining $\Sigma = \sqrt{\omega^2 - \gamma_0^2}$)

$$\bar{x}_t = \int_0^t ds \frac{1}{m\Sigma} e^{-\gamma_0(t-s)} \sin[(t-s)\Sigma] f_s, \quad (14)$$

is the mean position of the mirror, and

$$x_t^\xi = \int_0^t ds \frac{1}{m\Sigma} e^{-\gamma_0(t-s)} \sin[(t-s)\Sigma] \xi_s, \quad (15)$$

corresponds to the fluctuating component of the position. As is explicit in the above equations, the mean position follows the driving force, while the fluctuating term depends on the thermal noise ξ_t and has zero average. The analogous decomposition for the velocity of the mirror reads

$$v_t = \bar{v}_t + v_t^\xi,$$

where the average velocity is given by

$$\begin{aligned} \bar{v}_t &= \int_0^t ds \frac{e^{-\gamma_0(t-s)}}{m} f_s \times \\ &\times \left(\cos[(t-s)\Sigma] - \frac{\gamma_0}{\Sigma} \sin[(t-s)\Sigma] \right) \end{aligned} \quad (16)$$

and the fluctuating component by

$$\begin{aligned} v_t^\xi &= \int_0^t ds \frac{e^{-\gamma_0(t-s)}}{m} \xi_s \times \\ &\times \left(\cos[(t-s)\Sigma] - \frac{\gamma_0}{\Sigma} \sin[(t-s)\Sigma] \right). \end{aligned} \quad (17)$$

For later purposes, we note that $\mathbb{E}[v_t] = \bar{v}_t$, $\mathbb{E}[v_t^\xi] = 0$,

$$\mathbb{E}[v_t^2] = (\bar{v}_t)^2 + \mathbb{E} \left[\left(v_t^\xi \right)^2 \right] + 2\bar{v}_t \mathbb{E} \left[v_t^\xi \right],$$

and

$$\lim_{t \rightarrow \infty} \mathbb{E} \left[\left(v_t^\xi \right)^2 \right] = \frac{k_B T}{m}, \quad (18)$$

where we have used the noise time-correlation function $\mathbb{E} [\xi_t \xi_s] = 2\gamma k_B T \delta(t - s)$.

Stochastic energetics of the mirror. The power delivered by the engine can be determined from the stochastic energetics of the mirror.

The total internal energy of the mirror is given by

$$U_t = \frac{m}{2} v_t^2 + \frac{m \omega^2}{2} x_t^2,$$

and its derivative reads, using Eq. (13),

$$\frac{d}{dt} U_t = -\gamma v_t^2 + f_t v_t + v_t \xi_t.$$

Taking the average over all realizations, and considering a time large enough so that we can neglect transient behaviour and use the result of Eq. (18) we obtain

$$\frac{d}{dt} \mathbb{E} [U_t] = \gamma \frac{k_B T}{m} + f_t \bar{v}_t - \gamma \mathbb{E} [v_t^2]. \quad (19)$$

This equation shows that the variation of the energy balance of the mirror involves three components: the power delivered by the many-body quantum engine through the force f_t , the average power uptake from thermal fluctuations, which is proportional to the temperature T , and the energy that is dissipated by mechanical friction.

When the long-time dynamics of the mirror settles to an asymptotic cycle, we can compute the average power per cycle as

$$P_{\text{av}} = \frac{1}{t_c} \int_0^{t_c} dt f_t v_t = \frac{\gamma}{t_c} \int_0^{t_c} dt \left(\mathbb{E} [v_t^2] - \frac{k_B T}{m} \right),$$

where t_c is the period of the cycle. Using relation (18), this expression can be rewritten solely in terms of the mean velocity of the mirror

$$P_{\text{av}} = \frac{\gamma}{t_c} \int_0^{t_c} dt \bar{v}_t^2.$$

When the force f_t does not have an a priori known period, we can determine the delivered power through the long-time average

$$P_{\text{av}} = \lim_{t_{\text{obs}} \rightarrow \infty} \frac{\gamma}{t_{\text{obs}}} \int_0^{t_{\text{obs}}} dt \bar{v}_t^2.$$

This formula for the average power is justified by the fact that the energy of the mirror remains bounded and thus the average energy variation goes to zero at long times,

$$\lim_{t_{\text{obs}} \rightarrow \infty} \frac{1}{t_{\text{obs}}} (\bar{U}_{t_{\text{obs}}} - \bar{U}_0) = 0.$$

Hence, the energy absorbed by the mirror from the engine goes into an extra contribution of heat dissipated by friction, which adds to the equilibrium thermal one.

Numerical simulation of the engine dynamics and of the mirror. In order to quantitatively analyse the performance of our engine, we need to devise a suitable numerical scheme. In practice, we want to determine a system of differential equations involving dimensionless variables which are representative of the engine-mirror dynamics. To this end, we focus on the mean contribution of the position and of the velocity, which determine the power output.

We first define the dimensionless time $\tau = \omega t$. Next we consider the deterministic force which drives the mirror dynamics; this term is given, in the finite-density limit, by Eq. (11). By expressing it as a function of τ , we obtain

$$f_{t=\tau\omega^{-1}} = \hbar \omega_{\text{cav}}^0 D_0 F_\tau,$$

where we have extracted the dimensionless force

$$F_\tau = \frac{g}{\kappa} (\Gamma_0 s_+ s_-)_\tau. \quad (20)$$

This term depends on the atomic variables s_\pm at the time $\tau = t\omega$, as well as on the value of Γ_0 at τ , which is a function of the control parameter Δ . The values of s_\pm and s_z are determined by the system of differential equations

$$\begin{aligned} \frac{d}{d\tau} s_+ &= -i \frac{\Omega}{\omega} s_z - i \frac{\Delta}{\omega} s_+ - i \frac{g}{\omega} C_0 s_z s_+ + \frac{g}{\omega} \frac{\Gamma_0}{2} s_z s_+, \\ \frac{d}{d\tau} s_z &= 2i \frac{\Omega}{\omega} (s_- - s_+) - 2 \frac{g}{\omega} \Gamma_0 s_+ s_- . \end{aligned} \quad (21)$$

The mean position of the mirror \bar{x}_t , which appears in Eq. (14), can also be factorized into a dimensionless dynamical quantity and a dimensional constant depending on the details of the experimental setting,

$$\bar{x}_{t=\tau\omega^{-1}} = \frac{\omega_{\text{cav}}^0}{\omega} \frac{\hbar D_0}{m\omega} X_\tau, \quad (22)$$

where

$$X_\tau = \int_0^\tau dy \frac{\omega}{\Sigma} e^{-\frac{\gamma_0}{\omega}(\tau-y)} \sin \left[(\tau-y) \frac{\Sigma}{\omega} \right] F_y$$

and $\gamma_0 = \gamma/(2m)$. Similarly, the mean velocity of the mirror (16) can be expressed as

$$\bar{v}_{t=\tau\omega^{-1}} = \frac{\omega_{\text{cav}}^0}{\omega} \frac{\hbar D_0}{m} V_\tau, \quad (23)$$

where

$$\begin{aligned} V_\tau &= \int_0^\tau dy e^{-\frac{\gamma_0}{\omega}(\tau-y)} F_y \times \\ &\times \left\{ \cos \left[(\tau-y) \frac{\Sigma}{\omega} \right] - \frac{\gamma_0}{\Sigma} \sin \left[(\tau-y) \frac{\Sigma}{\omega} \right] \right\}. \end{aligned}$$

The quantities X_τ, V_τ are solution to the system of differential equations

$$\frac{d}{d\tau} \begin{pmatrix} X_\tau \\ V_\tau \end{pmatrix} = \begin{pmatrix} 0 & 1 \\ -1 & -2\gamma_0/\omega \end{pmatrix} \begin{pmatrix} X_\tau \\ V_\tau \end{pmatrix} + \begin{pmatrix} 0 \\ F_\tau \end{pmatrix}. \quad (24)$$

From the equations (20)-(24) the trajectory of the mirror can be determined numerically. The power that is delivered by the engine to the mirror can then be obtained from the relation

$$\begin{aligned} P_{\text{av}} &= \frac{\gamma}{t_{\text{obs}}} \int_0^{t_{\text{obs}}} dt \bar{v}_t^2 \\ &= \left(\frac{\omega_{\text{cav}}^0}{\omega} \right)^2 \frac{\hbar^2 D_0^2 \omega}{m} \left[2\gamma_0 \frac{1}{\tau_{\text{obs}}} \int_0^{\tau_{\text{obs}}} d\tau V_\tau^2 \right], \end{aligned} \quad (25)$$

where t_{obs} is the observation time, which equals the period of the driving $t_{\text{obs}} = 2\pi/\omega$ for the periodic mode of operation and is taken to be very large for the time-crystal mode, $t_{\text{obs}} \gg \omega^{-1}$.

Note that the rescaling of dynamical quantities keeps our analysis general and thus applicable to different experimental instances where $\omega_{\text{cav}}^0, \omega$, the mass of the mirror and the linear density of atoms can vary.

SUPPLEMENTARY INFORMATION

Effective Description and first-order expansion in x/L_0

A reduced dynamical description of the ensemble of atoms can be obtained by adiabatically eliminating the cavity light field [17, 36, 37]. In this section, we review this procedure and discuss the resulting dynamical generator.

The Heisenberg equation of motion for the bosonic operator a reads

$$\dot{a} = (i\delta - \frac{\kappa}{2})a - i\frac{g}{\sqrt{N}}S_- ,$$

and its formal solution is given by

$$a = e^{(i\delta - \frac{\kappa}{2})t}a_0 - i\frac{g}{\sqrt{N}} \int_0^t du e^{(i\delta - \frac{\kappa}{2})(t-u)}(S_-)_u .$$

In the adiabatic limit, where the operators S_{\pm} in the Heisenberg picture are practically constant on the relaxation time scale $1/\kappa$, this expression can be simplified to

$$a \approx -i\frac{g}{\sqrt{N}}S_- \int_0^t du e^{(i\delta - \frac{\kappa}{2})(t-u)} \approx \frac{-2igS_-}{\sqrt{N}(\kappa - 2i\delta)} ,$$

where $S_- = (S_-)_{u=t}$. Hence, the bosonic operator can effectively be replaced with the rescaled collective spin operator

$$a = \frac{2g}{\sqrt{N}(2\delta + i\kappa)}S_- . \quad (\text{S1})$$

Substituting this result into the total Hamiltonian of the system,

$$H_{\text{tot}} = H_{\text{L}} + H_{\text{int}} + H_{\text{ph}} ,$$

yields the effective Hamiltonian

$$\tilde{H} = H_{\text{L}} + \frac{g\hbar}{N} C S_+ S_- , \quad \text{with} \quad C = \frac{4g\delta}{4\delta^2 + \kappa^2} .$$

For the effective dissipator we obtain

$$\tilde{\mathcal{D}}[\rho] = \frac{g\hbar}{N} \Gamma \left(S_- \rho S_+ - \frac{1}{2} \{S_+ S_-, \rho\} \right) , \quad \text{with} \quad \Gamma = \frac{4g\kappa}{4\delta^2 + \kappa^2} .$$

Having derived an effective model for the ensemble of atoms, we now have to account for small oscillations of the mirror around its equilibrium position. Changing the length of the cavity alters the wave-length, and thus the frequency $\omega_{\text{cav}} = nc/(2L)$, of the light mode, where c denotes the speed of light and n is a positive integer. Hence the parameter $\delta = \omega_{\text{at}} + \Delta - \omega_{\text{cav}}$, which enters the effective Hamiltonian and the effective dissipation super operator, becomes a function of the the length $L = L_0 + x$.

For small oscillations, i.e., $x/L_0 \ll 1$, we have

$$\omega_{\text{cav}} = \frac{nc}{2(L_0 + x)} \approx \omega_{\text{cav}}^0 \left[1 - \frac{x}{L_0} \right] \quad \text{with} \quad \omega_{\text{cav}}^0 = \frac{nc}{2L_0} ,$$

and

$$\delta \approx \delta_0 + \omega_{\text{cav}}^0 \frac{x}{L_0} \quad \text{with} \quad \delta_0 = \omega_{\text{at}} + \Delta - \omega_{\text{cav}}^0 .$$

Consequently, the dimensionless constants Γ and C become

$$\Gamma \approx \Gamma_0 - \Gamma_1 \frac{x}{L_0}, \quad \text{with} \quad \Gamma_0 = \frac{4g\kappa}{\kappa^2 + 4\delta_0^2}, \quad \text{and} \quad \Gamma_1 = \omega_{\text{cav}}^0 \Gamma_0 \frac{8\delta_0}{(4\delta_0^2 + \kappa^2)},$$

and

$$C \approx C_0 - C_1 \frac{x}{L_0}, \quad \text{with} \quad C_0 = \frac{4g\delta_0}{\kappa^2 + 4\delta_0^2}, \quad \text{and} \quad C_1 = \frac{\omega_{\text{cav}}^0}{\delta_0} C_0 \frac{(4\delta_0^2 - \kappa^2)}{(4\delta_0^2 + \kappa^2)}.$$

These relations show how the reduced dynamical description of the atoms depends on the displacement of the mirror x .

By following the same lines, we find that the force acting on the mirror is given by

$$f_t = -\left\langle \left[\frac{\partial}{\partial x} H_{\text{ph}}^S \right] \right\rangle_t \approx \frac{\omega_{\text{cav}}^0}{L_0} \langle a^\dagger a \rangle_t \approx \frac{\hbar g}{N} \frac{\omega_{\text{cav}}^0}{\kappa L_0} \left(\Gamma_0 - \Gamma_1 \frac{x}{L_0} \right) \langle S_+ S_- \rangle_t.$$

where we have used the relation (S1) to eliminate the operators pertaining to the light field.

Dynamics in the finite density of atoms case.

In this section, we provide further details on how the non-linear differential equations, which govern the dynamics of the collective variables s_\pm and s_z , can be obtained from the effective description of the atomic system in the limit of finite density.

The Heisenberg equation of motion for the rescaled operator S_+/N is given by

$$\frac{d}{dt} \frac{S_+}{N} = i \left[H_{\text{eff}}, \frac{S_+}{N} \right] + \frac{g_0}{N} \frac{\Gamma_0}{2} \left(\left[S_+, \frac{S_+}{N} \right] S_- + S_+ \left[\frac{S_+}{N}, S_- \right] \right) = -i\Omega \frac{S_z}{N} - i\Delta \frac{S_+}{N} - i\frac{g}{N} C_0 \frac{S_z}{N} \frac{S_+}{N} + \frac{g\Gamma_0}{2} \frac{S_z}{N} \frac{S_+}{N}. \quad (\text{S2})$$

We now take the average of both sides of this differential equation with respect to the initial state ρ_0 of the atomic system and observe that quadratic contributions can be factorized as

$$\left\langle \frac{S_z}{N} \frac{S_+}{N} \right\rangle \longrightarrow \left\langle \frac{S_z}{N} \right\rangle \left\langle \frac{S_+}{N} \right\rangle \quad (\text{S3})$$

for $N \gg 1$, since the coupling between individual constituents of the ensemble is of order $1/N$. This approximation becomes exact in the limit $N \rightarrow \infty$ [42]. Furthermore, this scheme naturally extends to breaking up the time-evolution into a series of intervals with constant dynamical generator, which is the case for the quenched protocol adopted for the detuning Δ .

Using the relation (S3) and defining

$$s_\pm = \lim_{N \rightarrow \infty} \left\langle \frac{S_\pm}{N} \right\rangle, \quad s_z = \lim_{N \rightarrow \infty} \left\langle \frac{S_z}{N} \right\rangle,$$

yields the non-linear differential equation

$$\dot{s}_+ = -i\Omega s_z - i\Delta s_+ - igC_0 s_z s_+ + \frac{g\Gamma_0}{2} s_z s_+.$$

Along the same lines, we find the equation of motion for s_z ,

$$\dot{s}_z = 2i\Omega (s_- - s_+) - 2g\Gamma_0 s_+ s_-.$$